Radiology: Cardiothoracic Imaging

Extension of Coronavirus Disease 2019 (COVID-19) on Chest CT and Implications for Chest Radiograph Interpretation

Hyewon Choi, MD[1*]; Xiaolong Qi, MD[2*]; Soon Ho Yoon, MD, PhD[1]; Sang Joon Park, PhD[1]; Kyung Hee Lee, MD, PhD[3]; Jin Yong Kim, MD, MSc[4]; Young Kyung Lee, MD, PhD[5]; Hongseok Ko, MD[6]; Ki Hwan Kim, MD[7]; Chang Min Park, MD, PhD[1]; Yun-Hyeon Kim, MD, PhD[8]; Junqiang Lei, MD[2]; Jung Hee Hong, MD[1]; Hyungjin Kim, MD, PhD[1]; Eui Jin Hwang, MD, PhD[1]; Seung Jin Yoo, MD[1]; Ju Gang Nam, MD1; Chang Hyun Lee, MD, PhD[1]; Jin Mo Goo, MD, PhD[1]

*H.C. and X.Q. contributed equally to this work.

[1]Department of Radiology, Seoul National College of Medicine, Seoul National University Hospital, Seoul, Korea

[2]CHESS Center, The First Hospital of Lanzhou University, Lanzhou, China

[3]Department of Radiology, Seoul National University Bundang Hospital, Gyeonggi-do, Korea

[4]Department of Internal Medicine, Incheon Medical Center, Incheon, Korea

[5]Department of Radiology, Seoul Medical Center, Seoul, Korea

[6]Department of Radiology, National Medical Center, Seoul, Korea

[7]Department of Radiology, Myongji Hospital, Gyeonggi-do, Korea

[8]Department of Radiology, Chonnam National University Hospital, Gwanju, Korea

Type of manuscript: Original article

Corresponding Author: Soon Ho Yoon, MD, PhD

Department of Radiology, Seoul National University College of Medicine

Seoul National University Hospital

101 Daehak-ro, Jongno-gu, Seoul, 03080, Korea

E-mail: yshoka@gmail.com

Conflicts of interest:

Jin Mo Goo—not related to this article: Research Grant, Infinitt Healthcare; Research Grant, Dongkook Lifescience

Hyungjin Kim-- not related to this article: research grant from Lunit

Abbreviations: CT=computed tomography, COVID-19=coronavirus disease 2019, GGO=ground-glass opacity; AP=anteroposterior.

Key Points

1. In COVID-19 patients, considerable variation was found in the QCT_{mass} (72.4±120.8 g; range, 0.7–420.7 g) and relative 3D opacity extent on CT (3.2±5.8% of lung area; range, 0.1–19.8%).

2. Chest radiographs in patients under investigation for COVID-19 provided a sensitivity of 25% (5/20) and specificity of 90% (18/20) for COVID-19-related opacities.

3. The QCT_{mass} ($p<.001$) and the 3D opacity volume on CT ($p<.001$) significantly affected the visibility of COVID-19-related opacities on radiographs.

Summary Statement

Quantitative opacity mass and 3D opacity volume on CT were quantifiable metrics affecting the visibility of COVID-19-related opacities on chest radiographs.

Abstract

Purpose: To study the extent of pulmonary involvement in COVID-19 with quantitative CT (QCT) and to assess the impact of disease burden on opacity visibility on chest radiographs.

Materials and Methods: This retrospective study included 20 pairs of CT scans and same-day chest radiographs from 17 patients with COVID-19, along with 20 chest radiographs of controls. All pulmonary opacities were semi-automatically segmented on CT images, producing an anteroposterior projection image to match the corresponding frontal chest radiograph. The lung opacification mass (QCT_{mass}) was defined as [(opacity attenuation value+1000 HU)/1000]*1.065(g/mL) * combined volume (cm^3) of the individual opacities. Eight thoracic radiologists reviewed the 40 radiographs, and a receiver operating characteristics curve analysis was performed for the detection of lung opacities. Logistic regression analysis was done to identify factors affecting opacity visibility on chest radiographs.

Results: The mean QCT_{mass} per patient was 72.4±120.8 g (range, 0.7-420.7), and opacities occupied 3.2±5.8% (range, 0.1-19.8) and 13.9±18.0% (range, 0.5-57.8) of the lung area on the CT images and projected images, respectively. The radiographs had a median sensitivity of 25% and specificity of 90% among radiologists. Nineteen of 186 opacities were visible on chest radiographs, and a median area of 55.8% of the projected images was identifiable on radiographs. Logistic regression analysis showed that QCT_{mass} ($p<0.001$) and combined opacity volume ($p<0.001$) significantly affected opacity visibility on radiographs.

Conclusion: QCT_{mass} varied among COVID-19 patients. Chest radiographs had high specificity for detecting lung opacities in COVID-19, but a low sensitivity. QCT_{mass} and combined opacity volume were significant determinants of opacity visibility on radiographs.

Introduction

In December 2019, an outbreak of coronavirus pneumonia developed in the city of Wuhan, Hubei Province, China, with evidence of human-to-human transmission. Severe acute respiratory syndrome coronavirus 2 (SARS-CoV-2) was identified as the causative agent (1) of Coronavirus Disease 2019 (COVID-19), which became a pandemic infection. As of mid-March, over 150,000 cases have been confirmed globally and the total number of cases and deaths outside China has overtaken the total number of cases and deaths in China (2). Most of the infected patients presented with fever, respiratory symptoms, and pulmonary opacities on CT; 20% to 30% of the patients required mechanical ventilation, with death subsequently occurring in up to 10% of patients in some reports (3). A minor proportion of the patients that did not have clinical or radiologic abnormalities still served as a source of transmission (4).

The radiologic manifestations of COVID-19 have been mainly investigated on chest CT, and the typical findings were bilateral predominant ground-glass opacities (GGO) with or without consolidation in the peripheral lungs (5-7). The recognition of the typical CT findings of COVID-19 is particularly important for diagnosing the disease in patients under investigation with a negative result on real-time reverse-transcription polymerase-chain-reaction (PCR) assay (8, 9). Nevertheless, a minority of patients with COVID-19 have negative CT findings or unilobar abnormalities with a minimal extent, indicating a heterogeneous distribution of the disease.

Chest radiography is the primary imaging modality for evaluating acute respiratory illness in immunocompetent patients (10). Although COVID-19 can present with evident abnormalities on chest radiographs (1), in approximately two-thirds of the patients, radiographs were normal (11). The primary utilization of CT scans instead of chest radiographs might be suggested for evaluating suspected cases of COVID-19 based on the presumed higher sensitivity of the former. Nevertheless, it is operationally more complex to perform CT scans of suspected cases than chest radiographs, considering the preventive measures necessary to prevent the spread of the infectious agent (e.g., disinfection of imaging resources). Therefore, it is necessary to understand the diagnostic performance of chest

radiographs in comparison with CTs in COVID-19. This study aimed compared the detectability of pulmonary opacities on chest radiographs of patients with COVID-19, correlating these findings with quantitative measurements obtained by CT.

Materials and Methods

A part of the study population was included in another study that qualitatively analyzed the chest radiologic and CT findings of COVID-19 in Korea (9 of 14 patients) (12). The institutional review board of all participating institutions (Seoul National University Hospital, Seoul National University Bundang Hospital, Incheon Medical Center, Seoul Medical Center, and The First Hospital of Lanzhou University) approved this retrospective study, and the requirement for informed consent was waived.

Study population

There were 17 patients (mean age, 45.0±16.5 years; male-to-female ratio, 10:7) from 5 hospitals in Korea and China (14 patients from Korea and 3 patients from China) with PCR-proven COVID-19, who underwent a diagnostic chest CT scan and had an available same-day chest radiograph. One patient eventually required mechanical ventilation support during hospitalization; otherwise, patients recovered uneventfully. Thirteen of the patients underwent CT once at baseline, and the other four patients underwent CT twice (at baseline and follow-up). After excluding one normal baseline CT scan, we analyzed 20 CT scans and the corresponding chest radiographs of the patients. To analyze the diagnostic accuracy of chest radiographs for lung opacification caused by COVID-19, we additionally collected 20 chest radiographs as controls from 20 patients at a single hospital, who were under investigation for COVID-19 (mean age, 32.0±13.7 years; male-to-female ratio, 9:11), but who had both negative PCR and chest radiographs.

Image acquisition

All noncontrast CT scans were obtained in the supine position at full inspiration using a multi-detector CT scanner with 16 or more detector channels (Emotion 16, Somatom Sensation 64, Somatom Definition, Somatom Definition AS+, and Somatom Force [Siemens Healthineers, Erlangen, Germany]). The CT tube voltage and current were 120 kVp and a standard-dose or low-dose setting

with automatic exposure control was used according to institutional protocols. Axial CT images were reconstructed with a slice thickness of 1 mm (3 mm in a minority of the cases) and a sharp reconstruction kernel. Chest radiographs were obtained using the following devices: DRX-Revolution (Carestream Health, Rochester, NY, USA); Optima XR220 (GE Healthcare, Chicago, IL, USA); Fluorospot Compact FD (Siemens Healthcare, Erlangen, Germany); and CXDI (Canon Inc., Tokyo, Japan). All chest radiographs consisted of single frontal view. Fourteen chest radiographs were taken at upright position with posteroanterior projection and the remaining were taken with anteroposterior projection in supine position or sitting position.

Quantitative CT analysis

After uploading CT images from each patient to commercially available segmentation software (MEDIP PRO v2.0.0.0, MEDICALIP Co. Ltd., Seoul, Korea), a deep neural network (MEDIP PRO v2.0.0.0, MEDICALIP Co. Ltd., Seoul, Korea), automatically generated a volumetric mask of the lungs, lobes, intrapulmonary vessels, and airways. An image technician made a tentative volumetric opacity mask by applying a variable density mask based on CT attenuation thresholds to contain the entire opacity. Then, the pulmonary and airway masks were subtracted from the tentative mask. The mask containing the entire opacity was separated by checking the connectivity across individual opacities, and the separated opacity masks were labeled in numerical order. A chest radiologist (S.H.Y, with 15 years of clinical experience of thoracic imaging) reviewed and confirmed the opacity masks. If any corrections were required, a manual adjustment was applied to the minimum extent necessary (**Figure 1A**). In addition, the radiologist recorded whether the individual opacities showed anteroposterior (AP) overlap with the heart or hilum, or if located below the diaphragmatic dome or above the top of the aortic arch on CT, as opacities in these locations often tend to be less visible on radiographs.

The mean attenuation values and 3D volumes were extracted based on the opacity masks from the CT scans. The quantitative CT opacity mass (QCT_{mass}) was defined as the density of lung opacities

multiplied by 1.065 (g/mL) (13) and by the combined 3D volume (cm^3) of the individual opacities in the whole CT scan. As lung opacities typically had attenuation values below zero, the attenuation values were converted to the density of lung tissue by adding 1,000 to the HU values of each voxel and dividing by 1,000 (13). The densities in the range from air (-1024 HU) to water (0 HU) were approximately equal to the physical densities (14), and the density of the lung tissue was assumed to be 1.065 g/mL (13).

Radiograph Interpretation

Eight thoracic radiologists (H.C., J.H.H., H.K., E.J.H., C.H.L., K.H.K., H.K., and J.M.G with 5 years to 23 years of clinical experience in thoracic imaging) reviewed 40 anonymized chest radiographs (20 radiographs of patients with COVID-19 and 20 control radiographs) in a random order. The readers independently rated the presence of opacities on the radiographs using a clinical picture archiving and communication system workstation, using a 5-point Likert scale (1, definitely absent; 2, probable absent; 3, uncertain; 4, probably present; 5, definitely present). They also recorded the location and type of each opacity (consolidation or GGO) when assigning a rating higher than 3.

Comparisons between CTs and Radiographs

The lung and opacity 3D masks (**Figure 1B**) on CT were displayed in different color renderings and viewed as a single image in the AP projection, enabling the estimation of the 2D area (cm^2) on chest radiographs (**Figure 1C**). A opacity on a CT image was considered to be visible on a chest radiograph if at least three of the eight readers agreed that it was probably or definitely present, and if the recorded location of the opacity on the chest radiograph matched the location of the projected image. In cases where opacities were visible, a radiologist (H.C) who was blinded to the CT images manually drew a free-hand region of interest on the chest radiographs.

Statistical analysis

The diagnostic performance of the readers on chest radiographs was evaluated through a receiver operating characteristic curve analysis, using with a Likert score for pulmonary opacity of 4 or 5 as evidence for COVID-19. The relationship between opacity 3D volume and 2D area was assessed by calculating the Pearson correlation coefficient (r). The quantitative parameters were compared using the Mann-Whitney test and the Fisher exact test according to the visibility of opacities on chest radiographs at the patient and lung level. Logistic regression analysis was conducted to evaluate factors affecting opacity visibility on chest radiographs at the opacity level. All statistical analyses were conducted using SPSS software (version 25.0, IBM Corp., Armonk, NY, USA).

Results

CT Opacification in COVID-19

A total of 186 opacities were identified in 20 patients, with an average number of 9.4±8.1 opacities per patient. **Table 1** shows the results of the quantitative CT analysis in the 20 patients with COVID-19. The mean QCT_{mass} per patient was 72.4±120.8 g (range, 0.7 to 420.7 g). The mean relative 3D extent of opacities in the lung parenchyma per patient was 3.2±5.8% of the total lung volume (range, 0.1% to 19.8%). The mean CT attenuation of all opacities per patient was -448.2±173.1 HU (range, -777.0 to -127.0 HU). The mean QCT_{mass} per opacity was 7.3±19.5 g (range, 0.005 to 111.9 g). The mean attenuation per opacity was -492.4±168.8 HU (range, -816.0 to -126.0 HU). The mean 3D volume of the opacities was 13.2±35.2 cm^3 (range, 0.02 to 185.8 cm^3).

Reader Performance for Detecting COVID-19-related Opacities on Chest Radiographs

The median sensitivity among readers was 25% (interquartile range [IQR], 20% to 26.3%), and the median specificity was 90% (IQR, 88.8% to 96.3%) with a median area under the curve of 0.575 (range, 0.525 to 0.725) (**Figure 2**). Four of the 20 chest radiographs with opacities on CT were correctly diagnosed by all readers, and nine chest radiographs with opacities on CT were missed by all readers. The median number of positive calls on chest radiographs was four (IQR, 3 to 4.75).

Lung Area and Relative Opacity Extent on AP Projection View

On AP projections of the CT images, the average relative opacity extent per patient was 13.9±18.0% (range, 0.5% to 57.8%). In the 20 patients, the Pearson correlation coefficient between the 2D area on the AP projection view and the 3D volume on chest CT was 0.978 on a per-patient basis and 0.901 on a per-opacity basis ($p<.001$). The correlation coefficient between the 2D area on the AP projection view and the QCT_{mass} was 0.878 on a per-patient basis and 0.847 on a per-opacity basis (all $p<.001$) (**Figure 3**).

Comparison between Visible and Invisible Opacities on Chest Radiographs

Nineteen of the 186 opacities were detected on chest radiographs. The median proportion between the identifiable opacity area on the chest radiograph to the projected opacity area based on CT was 55.8% (IQR, 49.9% to 57.1%). On a per-patient basis, the visible opacities on chest radiographs showed a significantly greater opacity extent and QCT_{mass} than did the invisible opacities ($p<.033$ and $p<.025$, respectively). Five of the six COVID-19 patients (83.3%) with a CT extent larger than 2% or a QCT_{mass} of greater than 55 g had visible opacities on radiographs.

On a per-lung basis, there were significant differences in the number of involved lobes, the number of opacities, the opacity extent, and the QCT_{mass} ($p<.027$, $p<.020$, $p<.001$, and $p<0.001$, respectively). Visible opacities on chest radiographs were detected in 87.5% (7 of 8) with a QCT_{mass} greater than 55 g, and in 100% (7 of 7) of the lungs with a relative volume extent exceeding 4%. There were no significant differences in the mean attenuation between the visible and invisible opacities on both a per-patient and a per-lung basis ($p<.933$ and $p<.636$, respectively) (**Table 3**).

Predictive Factors of Opacity Visibility on Chest Radiographs

Logistic regression analysis showed that the QCT_{mass} ($p<.001$) and 3D opacity volume ($p<.001$) significantly affected the visibility of opacities on chest radiographs (**Table 4**), whereas no significant differences in opacity visibility were found according the mean opacity attenuation value ($p=.618$) or if the opacity was located in a predetermined less visible region ($p=.309$).

Discussion

In the current study, we performed a quantitative CT analysis to assess the radiologic burden of COVID-19. The mean attenuation of pulmonary opacities was -492.4±168.8 HU, and the attenuation was in accordance with the qualitative CT findings reported in the literature, according to which COVID-19 typically manifests as predominant GGO (6, 7). The QCT_{mass} and 3D opacity extent on CT per patient ranged widely, from 0.7g to 420.7g and from 0.1% to 19.8%, respectively, which is in line with observations of a diverse spectrum of disease severity in COVID-19. The diverse radiologic burden in COVID-19 cases with similar radiologic findings indicates that a simple qualitative description of CT findings (i.e., predominant GGO in the peripheral lung) may be insufficient for the proper patient management.

The prevention of transmission and quarantine of infected patients are vital components of the management of COVID-19. Chest CT was extensively used for diagnosis and monitoring of patients under investigation for COVID-19 in China. Nevertheless, utilizing chest CT as the primary imaging modality for all suspected cases of COVID-19 has logistical limitations, in that disease is thought to spread from person to person, leading to time-consuming disinfection procedures and undesirable downtime of CT facilities, potentially overwhelming the capacity of radiological services. On the other hand, though chest radiography is a more flexible imaging modality, widely available globally, the assessment of its performance in a head-to-head comparison with CT in COVID-19 was lacking. We found in this study that chest radiographs were remarkably less sensitive for detecting COVID-19-related lung opacities, despite its high specificity. Depending on the probability of infection in suspected cases of COVID-19, the use of chest radiography and CT scans can be appropriately balanced in each institution, considering the available resources of health care personnel, medical facility, and disinfection procedures versus the lower diagnostic performance of the former imaging method.

Opacities were not only under detected on chest radiographs, but also underestimated in size when compared with CT. Only about 56% of the opacities on the projected image were actually seen on radiographs. We found that the extension of disease was the main factor driving the visibility of lung

opacities on chest radiographs. Therefore, clinicians and radiologists should keep in mind that a greater extent of disease can exist than that suggested by inspection of chest radiographs, and that chest radiographs may also have limitations for monitoring the disease extent.

Our study has several limitations. First, the study population was relatively small. Second, as aforementioned, we solely evaluated the radiologic burden of COVID-19 and did not investigate correlations of radiologic findings with clinical manifestations or outcomes. Third, as cases were collected from multiple centers, the image quality and positioning of the chest radiographs were not consistent. Although such inconsistencies reflect real clinical practice, they may also have decreased the readers' performance. Fourth, although we excluded pulmonary vessels within the opacity as much as possible, residual intraopacityal vessels after segmentation may have increased the CT attenuation of opacities, potentially affecting the calculated QCT_{mass}.

In conclusion, chest radiographs had low sensitivity and high specificity for detecting COVID-19-related lung opacities. The QCT_{mass} and 3D opacity volume on CT, which are quantitative surrogates of disease extension, were significant determinants of opacity visibility on radiographs. It is crucial to properly understand the diagnostic accuracy and limitations of chest radiographs in COVID-19 to improve the quality of patient management by ensuring an appropriate balance between the practicality of chest radiography versus better diagnostic performance of CT scans.

Acknowledgment

The authors would like to acknowledge Andrew Dombrowski, PhD (Compecs, Inc.) for his assistance in improving the use of English in this manuscript.

References

1. Zhu N, Zhang D, Wang W, et al. A novel coronavirus from patients with pneumonia in China, 2019. N Engl J Med 2020;382:727-733. doi: 10.1056/NEJMoa2001017

2. World Health Organization, *Coronavirus Disease (COVID-19) Situation Reports – 56.* https://www.who.int/docs/default-source/coronaviruse/situation-reports/20200316-sitrep-56-covid-19.pdf?sfvrsn=9fda7db2_2. Published March 16, 2020.

3. Paules CI, Marston HD, Fauci AS. Coronavirus infections—more than just the common cold. JAMA 2020;323(8):707-708. doi:10.1001/jama.2020.0757

4. Yan Bai LY, Tao Wei, Fei Tian, Dong-Yan Jin, Liguan Chen, Meiyun Wang. Presumed Asymptomatic Carrier Transmission. JAMA **doi:**10.1001/jama.2020.2565. Published online February 21, 2020.

5. Kim JY, Choe PG, Oh Y, et al. The first case of 2019 novel coronavirus pneumonia imported into Korea from Wuhan, China: implication for infection prevention and control measures. J Korean Med Sci 2020;35(5):e61 **doi:**10.3346/jkms.2020.35.e61. Published online February 3, 2020.

6. Chung M, Bernheim A, Mei X, et al. CT imaging features of 2019 novel coronavirus (2019-nCoV). Radiology 2020;295:202-207. doi:10.1148/radiol.2020200370.

7. Kanne JP. Chest CT Findings in 2019 Novel Coronavirus (2019-nCoV) Infections from Wuhan, China: Key Points for the Radiologist. Radiology 2020;295:16-17. doi:10.1148/radiol.2020200241

8. Xie X, Zhong Z, Zhao W, Zheng C, Wang F, Liu J. Chest CT for Typical 2019-nCoV Pneumonia: Relationship to Negative RT-PCR Testing. Radiology. **doi:** 10.1148/radiol.2020200343. Published online February 12, 2020.

9. Fang Y, Zhang H, Xie J, et al. Sensitivity of Chest CT for COVID-19: Comparison to RT-PCR. Radiology. **doi**:10.1148/radiol.2020200343. Published online February 19, 2020.

10. Jokerst C, Chung JH, Ackman JB, et al. ACR Appropriateness Criteria® Acute Respiratory Illness In Immunocompetent Patients. Available at https://acsearch.acr.org/docs/69446/Narrative/.

11. Ng M-Y, Lee EY, Yang J, et al. Imaging Profile of the COVID-19 Infection: Radiologic Findings and Literature Review. Radiol Cariothorac Imaging **doi**:10.1148/ryct.2020200034. Published

online February 13, 2020.

12. Yoon SH, Lee KH, Kim JY, et al. Chest Radiographic and CT Findings of the 2019 Novel Coronavirus Disease (COVID-19): Analysis of Nine Patients Treated in Korea. Korean J Radiol. 2020;21:e24. **doi:**10.3348/kjr.2020.0132. Published online February 26, 2020.

13. Coxson HO, Rogers RM, Whittall KP, et al. A quantification of the lung surface area in emphysema using computed tomography. Am J Respir Crit Care Med 1999;159(3):851-6.

14. Hedlund LW, Vock P, Effmann EL. Evaluating lung density by computed tomography. In: Seminars in Respiratory Medicine: Thieme Medical Publishers, Inc., 1983; 76-88. doi: 10.1164/ajrccm.159.3.9805067.

Tables

Table 1. Quantitative CT analysis of segmented opacities

Case	No. of opacities	Location	Total lung volume (cm^3)	Total opacity volume (cm^3)	Extent of opacities (%)	Mean attenuation (HU) *	QCT_{mass} (g) †
1	12	RUL (4), RLL (3), LUL (3), LLL (2)	3716.9	28.6	0.8	-481.2 ± 151.6	38.1
2	6	RLL(3) LUL(2), LLL(1)	7937.5	26.6	0.3	-352.0 ± 170.1	30.0
3	1	LLL(1)	4489.1	7.4	0.2	-196.0	6.3
4	2	RLL(1), LUL(1)	2997.1	1.4	0.05	-497.0 ± 44.0	0.8
5	9	RUL(3), RML(1), RLL(1), LUL(3), LLL(1)	2936.7	581.6	19.8	-309.8 ± 63.2	420.7
6	15	RUL(1), RML(1), RLL (5), LUL (4), LLL(4)	6296.7	823.1	13.1	-714.5 ± 40.2	250.1
7	1	RLL(1)	5478.4	2.7	0.1	-777.0	0.7
8	2	RLL(1), LLL(1)	4920.0	21.2	0.4	-537.5 ± 51.5	9.3
9	22	RUL(4), RML (3), RLL(7), LUL (7) LLL (1)	4484.0	87.	1.9	470.1 ± 111.2	62.3
10	1	RLL(1)	5096.9	6.8	0.1	-280.0	5.2
11	4	RML(2), RLL(2)	7474.9	84.8	1.1	-666.8 ± 67.3	37.4
12	9	RML(2), RLL(6), LUL(1)	3323.2	69.5	2.1	-309.4 ± 127.5	54.8
13	33	RML(1) RLL(15), LUL(2), LLL(15)	5026.5	20.1	0.4	-642.2 ± 68.4	8.5
14	12	LUL(12)	5148.4	106.6	2.1	-488.9 ± 74.8	59.6
15	1	LLL(1)	3237.0	5.8	0.2	-127.0	5.4
16	12	RUL(5), RML(2),RLL(3), LUL(1), LLL(1)	4930.3	60.8	1.2	-398.8 ± 104.5	48.1
17	19	RUL(4), RML(3), RLL(3), LUL(6), LLL(3)	3890.5	675.5	17.4	-561.7 ± 39.9	353.0
18‡	13	RUL(4), RLL(5), LUL(2), LLL(2)	3751.6	24.2	0.7	-272.2 ± 120.3	20.9
19‡	7	LLL(7)	4960.3	17.1	0.3	-314.4 ± 57.5	12.8
20‡	6	RML(2), RLL(2), LLL(2)	4932.0	46.1	0.9	-567.5 ± 70.9	23.4

Notes – Data in parentheses are the number of opacities.
*Data are mean ± standard deviation.
†The QCT_{mass} was calculated as (mean attenuation + 1000)/1000*1.065*opacity volume (11).
‡Cases 18–20 are follow-up images of cases 1, 3, and 8, respectively.
RUL=right upper lobe; RML=right middle lobe; RLL=right lower lobe; LUL=left upper lobe; LLL=left lower lobe; QCT_{mass} = Quantitative CT opacity mass

Table 2. Visibility and proportion of identifiable opacities on anteroposterior projection images

Case	No. of opacities	Total lung area (cm^2)	Total opacity area (cm^2)	Extent of opacities (%)	Visibility on chest radiograph	Opacity area on chest radiograph (cm^2)	Opacity area on chest radiograph / Total opacity area on projected view (%)
1	12	466.4	36.4	7.8	-		
2	6	517.7	49.8	9.6	-		
3	1	563.0	5.7	1.0	+	5.7	100
4	2	453.7	2.1	0.5	-		
5	9	458.4	262.3	57.2	+	146.3	55.8
6	15	690.4	398.9	57.8	+	40.5	10.2
7	1	616.9	2.9	0.5	-		
8	2	597.5	15.5	2.6	-		
9	11	589.6	90.0	15.3	-		
10	1	563.9	10.5	1.9	-		
11	4	764.5	82.5	10.8	-		
12	9	425.0	66.5	15.7	-		
13	33	606.8	34.3	5.7	-		
14	12	583.7	59.2	10.1	+	26.5	49.9
15	1	463.1	6.3	1.4	-		
16	12	592.1	63.3	10.7	-		
17	19	486.6	246.6	50.7	+	140.7	57.1
18†	13	462.5	28.9	6.2	-		
19†	7	645.8	25.2	3.9	-		
20†	6	591.2	50.4	8.5	-		

Notes –
Visibility on chest radiography was determined when at least 3 of the 8 readers rated the radiograph as showing pneumonia.
†Cases 18–20 are follow-up images of cases 1, 3, and 8, respectively.

Table 3. Comparison between visible and invisible opacity on chest radiographs

	Per-patient analysis (n=20)			Per-lung analysis (n=40)		
	Visible opacity (n=5)	**Invisible opacity (n=15)**	**p-value**	**Visible opacity (n=8)**	**Invisible opacity (n=32)**	**p-value**
Bilaterality*	3	10	0.787	N/A	N/A	N/A
No. of involved lobes†	3.6 ± 1.7	2.7 ± 1.4	0.306	2.1 ± 0.8	1.3 ± 8.4	0.027
No. of opacities†	11.2 ± 6.1	8.7 ± 8.9	0.395	7.0 ± 7.5	3.8 ± 4.4	0.020
Mean attenuation (HU) †	-454.2 ± 183.3	-446.2 ± 175.4	0.933	-481.2 ± 195.2	-453.4 ± 156.1	0.636
Extent of opacity (%)†	10.5 ± 8.0	0.7 ± 0.6	0.033	13.2 ± 7.5	0.7 ± 0.9	<0.001
QCT_{mass} (g) †	217.9 ± 180.5	23.2 ± 20.3	0.025	136.2 ± 76.4	10.9 ± 15.8	<0.001

Notes – Data are mean ± standard deviation.
p-values were calculated using the Fisher exact test* and the Mann-Whitney test. †
QCT_{mass} = Quantitative CT opacity mass

Table 4. Logistic regression analysis of factors affecting opacity visibility on chest radiographs

	Odds ratio	95% CI	p-value*
Mean attenuation (HU)	0.999	0.996 – 1.002	0.618
QCT_{mass} (g)	1.092	1.054 – 1.131	<0.001
3D volume (cm^3)	1.000	1.000 – 1.000	<0.001
Less-visible opacity location†	1.740	0.598 – 5.061	0.309

Notes – Data are mean ± standard deviation.
p-values were calculated using logistic regression analysis.*
Less visible opacity locations† include locations that showed anteroposterior overlapped with the heart or hilum, or were below the diaphragmatic dome or above the top of the aortic arch on CT.
QCT_{mass} = Quantitative CT opacity mass

Figure legends

Figure 1. Coronal CT (A), volume/polygonal rendering (B), anteroposterior projection image (C), and anteroposterior chest radiograph (D) in a 55-year-old male patient with coronavirus disease 2019 pneumonia.

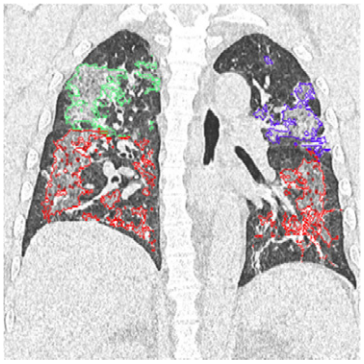

(A) A coronal CT image shows multiple mixed ground-glass opacities in both lungs. The boundaries of the pulmonary opacities are shown in color (right upper lobe, green; left upper lobe, blue, both lower lobes, red). Pneumonia involved 19.8% of the lung parenchymal area and the quantitative CT opacity mass was 420.7 g. The mean CT attenuation of pneumonia was -309.8±63.2 HU.

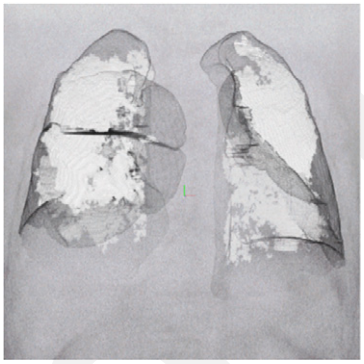

(B) A volume/polygonal rendering 3D image shows multiple opacity masks (white) in the mask of the right and left lobes (black boundary).

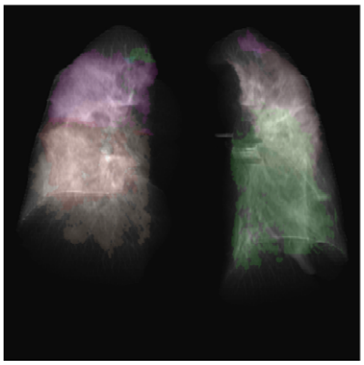

(C) An anteroposterior projection image shows multiple opacity masks in color that are overlaid on the right and left lobes in grayscale. The opacities involved 57.2% of the lung parenchymal area on the projected image.

(D) An anteroposterior chest radiograph shows multiple peripheral consolidation opacities in both lungs; 55.8% of the opacity masks in the projected image could be seen on the chest radiograph.

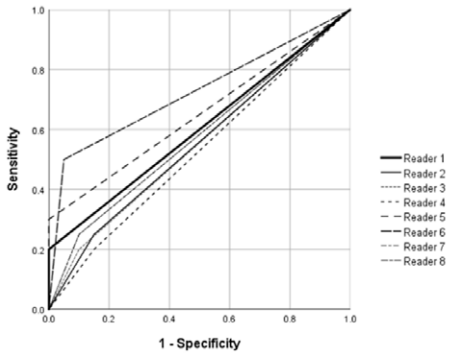

Figure 2. Receiver operating characteristic curve analysis of observer performance for detecting pneumonia

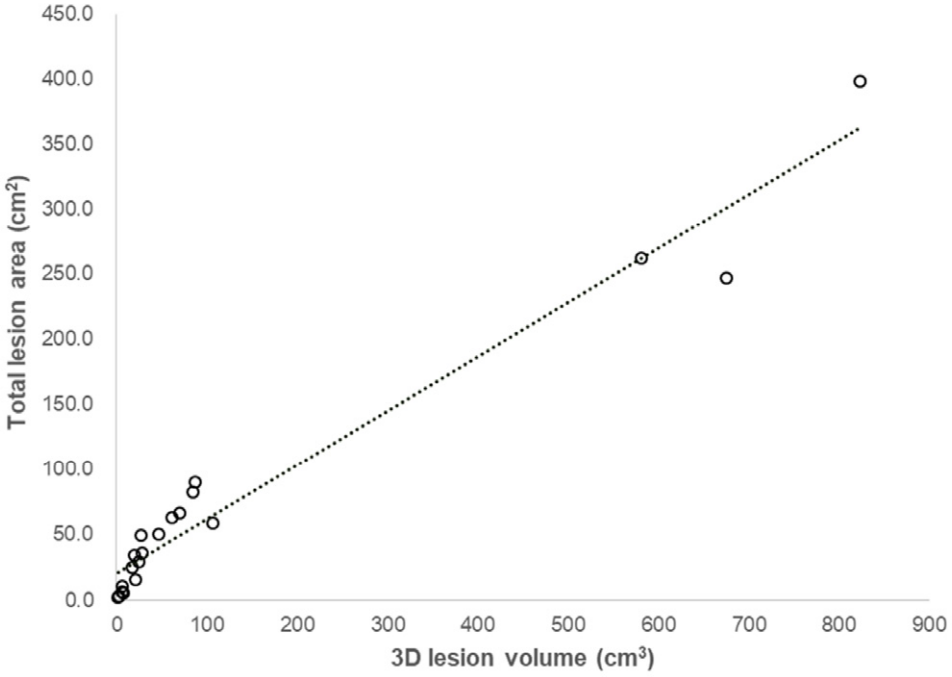
Total lesion area (cm²)
3D lesion volume (cm³)
0.0
50.0
100.0
150.0
200.0
250.0
300.0
350.0
400.0
450.0
0
100
200
300
400
500
600
700
800
900

3a.

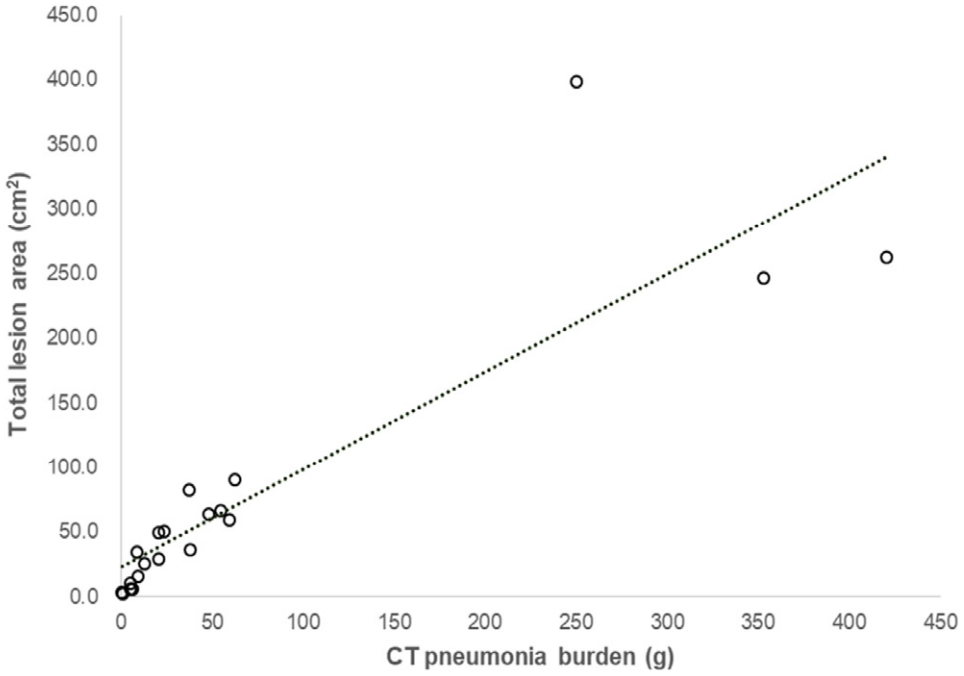
Total lesion area (cm²)
CT pneumonia burden (g)
0.0
50.0
100.0
150.0
200.0
250.0
300.0
350.0
400.0
450.0
0
50
100
150
200
250
300
350
400
450

3b.

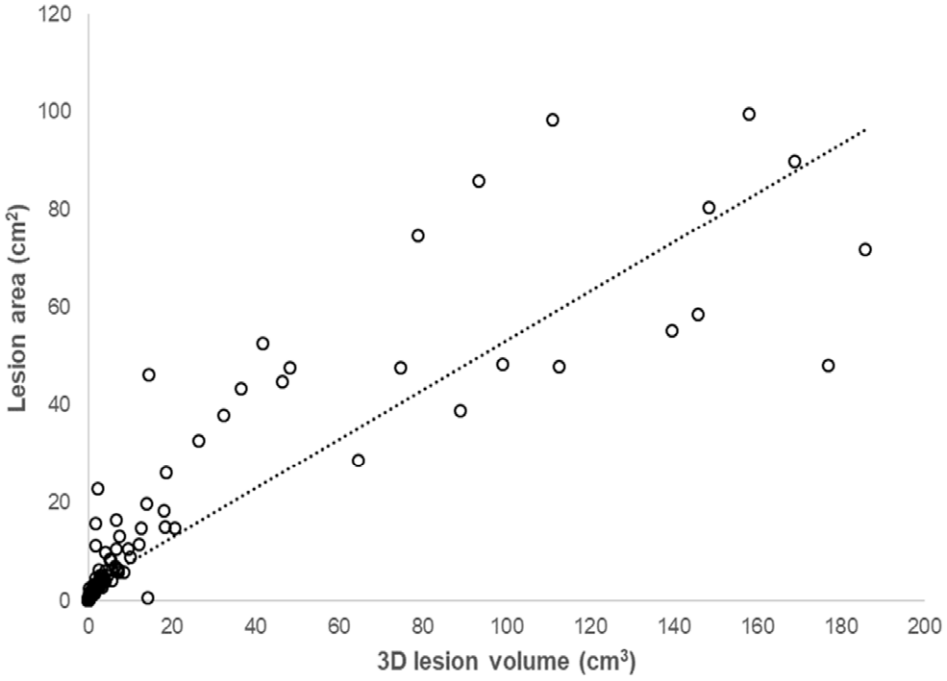
Lesion area (cm²)
3D lesion volume (cm³)
0
20
40
60
80
100
120
140
160
180
200

j

3c.

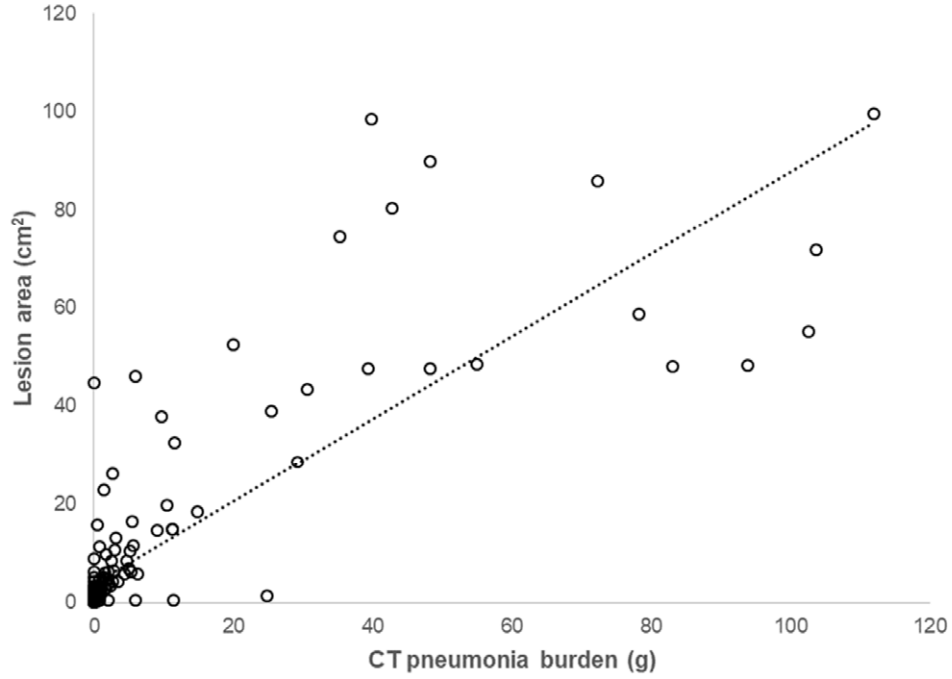
Lesion area (cm²)
CT pneumonia burden (g)
0
20
40
60
80
100
120

3d.

Figure 3. Scatter plots comparing the 2D opacity area (cm^2) and 3D volume (cm^3) and quantitative opacity mass (g) on CT on a per-patient (A, B) and per-opacity basis (C, D)

Supplemental materials

Supplemental figure 1. Coronal CT (A), volume/polygonal rendering (B), anteroposterior projection image (C), and chest anteroposterior radiograph (D) in a 28-year-old male patient with coronavirus disease 2019.

(A) A coronal CT image shows multiple mixed ground-glass opacities in the left upper lobe. The boundaries of the pulmonary opacities are shown in blue. Pneumonia involved 2.1% of the lung parenchymal area and the quantitative CT opacity mass was 59.6 g. The mean CT attenuation of pneumonia was -488.9±74.8 HU.

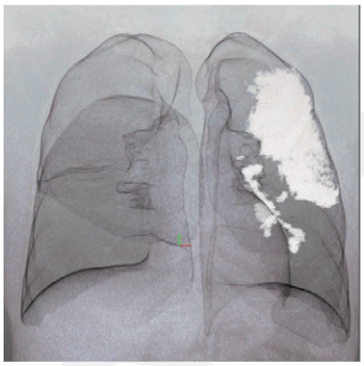

(B) A volume/polygonal rendering three-dimensional image shows multiple opacity masks (white) in the masks of the left lobes (black boundary).

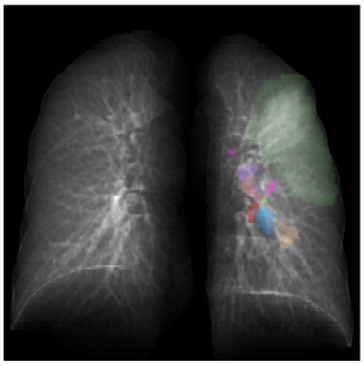

(C) An anteroposterior projection image shows multiple opacity masks in color that are overlaid on the right and left lobes in grayscale. The opacities involved 10.1% of the lung parenchymal area on the projected image.

(D) A posteroanterior chest radiograph shows a peripheral consolidation opacity in the left upper lung zone; 49.9% of the opacity masks in the projected image could be seen on the chest radiograph.

Supplemental figure 2. Coronal CT (A), volume/polygonal rendering (B), anteroposterior projection image (C), and chest anteroposterior radiograph (D) in a 53-year-old female patient with coronavirus disease 2019 pneumonia.

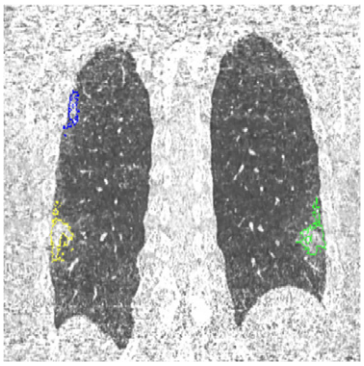

(A) A coronal CT image shows multiple mixed ground-glass opacities in both lower lobes. The boundaries of the pulmonary opacities are shown in color (right lower lobe superior segment, blue; right lower lobe lateral basal segment, yellow; left lower lobe lateral basal segment, green). Pneumonia involved 0.3% of the lung parenchymal area, and the quantitative CT opacity mass was 30.0 g. The mean CT attenuation of pneumonia was -352.0±170.1HU.

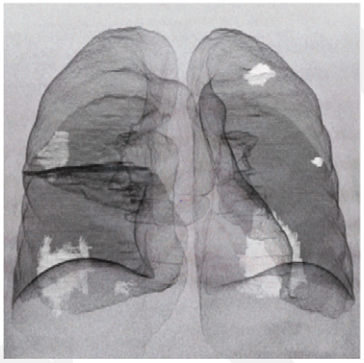

(B) A volume/polygonal rendering three-dimensional image shows multiple opacity masks (white) in the masks of the right and left lobes (black boundary).

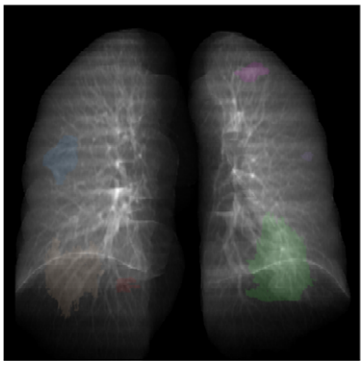

(C) An anteroposterior projection image shows multiple opacity masks in color that are overlaid on the right and left lobes in grayscale. The opacities involved 9.6% of the lung parenchymal area on the projected image.

(D) A normal anteroposterior chest radiograph, with no visible pneumonia.